European Radiology (2019) 29:1693–1702
https://doi.org/10.1007/s00330-018-5696-4

CHEST

Cardio-pulmonary MRI for detection of treatment response after a single BPA treatment session in CTEPH patients

Christian Schoenfeld[1,2] · Jan B. Hinrichs[1,2] · Karen M. Olsson[2,3] · Martin-Alexander Kuettner[1] · Julius Renne[1,2] · Till Kaireit[1,2] · Christoph Czerner[1,2] · Frank Wacker[1,2] · Marius M. Hoeper[2,3] · Bernhard C. Meyer[1,2] · Jens Vogel-Claussen[1,2]

Received: 6 May 2018 / Revised: 16 July 2018 / Accepted: 31 July 2018 / Published online: 11 October 2018

Abstract

Objectives Chronic thromboembolic pulmonary hypertension (CTEPH) can be treated with balloon pulmonary angioplasty (BPA) in inoperable patients. Sensitive non-invasive imaging methods are missing to detect treatment response after a single BPA treatment session. Therefore, the aim of this study was to measure treatment response after a single BPA session using cardio-pulmonary MRI.

Materials and methods Overall, 29 patients with CTEPH were examined with cardio-pulmonary MRI before and 62 days after their initial BPA session. Pulmonary blood flow (PBF), first-pass bolus kinetic parameters, and biventricular mass and function were determined. Multiple linear regression analysis was implemented to estimate the relationship of PBF change in the treated lobe with treatment change of full width at half maximum (FWHM), cardiac output (CO), ventricular mass index (VMI), pulmonary transit time (PTT) and PBF change in the non-treated lobes. Paired Wilcoxon rank sum test and Spearman rho correlation were used.

Results After BPA regional PBF increased in the treated lobe ($p < 0.0001$) as well as in non-treated lobes ($p = 0.015$). PBF treatment changes in the treated lobe were significantly larger compared with the non-treated lobes ($p = 0.0049$). Change in NT proBNP, MRI-derived mean pulmonary artery pressure (mPAP), PTT, FWHM, right ventricular (RV) ejection fraction, RV stroke volume, CO, VMI and PBF in the non-treated lobes correlated with PBF change in the treated lobe ($p < 0.05$). PBF changes in the treated lobe were independently predicted by PTT as well as PBF change in the non-treated lobes.

Conclusion Cardio-pulmonary MRI detects and quantifies treatment response after a single BPA treatment session.

Key Points

- *Two months after BPA regional parenchymal pulmonary perfusion (PBF) increased in the total lung parenchyma ($p = 0.005$), the treated lobes ($p < 0.0001$) and non-treated lobes ($p = 0.015$).*
- *The PBF treatment changes in the treated lobe were significantly larger than in the non-treated lobes ($p = 0.0049$).*
- *Change in NT proBNP, MRI-derived mean pulmonary artery pressure, pulmonary transit time, full width at half maximum, right ventricular (RV) ejection fraction, RV stroke volume, cardiac output, ventricular mass index and PBF in the non-treated lobes correlated with PBF change in the treated lobe ($p < 0.05$).*

Keywords Pulmonary hypertension · Balloon angioplasty · Perfusion · Heart · Magnetic resonance imaging

Christian Schoenfeld and Jan B Hinrichs contributed equally

✉ Jens Vogel-Claussen
vogel-claussen.jens@mh-hannover.de

[1] Institute for Diagnostic and Interventional Radiology, Hannover Medical School, OE 8220, Carl-Neuberg-Str. 1, 30625 Hannover, Germany

[2] Biomedical Research in Endstage and Obstructive Lung Disease Hannover (BREATH), Member of the German Center for Lung Research (DZL), Hannover, Germany

[3] Department of Respiratory Medicine, Hannover Medical School, Hannover, Germany

Abbreviations

6MWD	Six-minute walking distance
BPA	Balloon pulmonary angioplasty
BSA	Body surface area
CO	Cardiac output
CTEPH	Chronic thromboembolic pulmonary hypertension
DCE	Dynamic contrast enhanced
EDV	End-diastolic volume
EF	Ejection fraction
ESV	End-systolic volume
FWHM	Full width at half maximum
LV	Left ventricular
mPAP	Mean pulmonary artery pressure
NT-proBNP	N-terminal pro B-type natriuretic peptide
NYHA FC	New York Heart Association functional classification
PBF	Pulmonary blood flow
PE	Pulmonary embolism
PEA	Pulmonary endarterectomy
PH	Pulmonary hypertension
PTT	Pulmonary transit time
PVR	Pulmonary vascular resistance
RHC	Right-sided heart catheterization
RV	Right ventricular
SV	Stroke volume
TTP	Time to peak
TWIST	Time-resolved angiography with stochastic trajectories
VMI	Ventricular mass index

Introduction

Chronic thromboembolic pulmonary hypertension (CTEPH) is a life-threatening disease caused by persistent obstruction of pulmonary arteries as a result of residual pulmonary emboli and intraluminal post-embolic scar-tissue strictures [1–3]. It is potentially curable by pulmonary endarterectomy (PEA) [3, 4]. About 50% of CTEPH patients are not operable, and up to half undergoing pulmonary endarterectomy have residual pulmonary hypertension (PH), which occasionally requires additional treatment [5, 6]. These patients can be treated by drug therapy or more recently by balloon pulmonary angioplasty (BPA) [3]. The goal of this interventional technique is to eliminate the vascular obstruction by tearing and pressing the intraluminal post-embolic scar-tissue strictures in the form of bands or webs against the vascular walls [7]. Usually several single-lobe BPA sessions are performed using modern imaging technology and undersized balloons to minimize injury to the pulmonary vessels and to avoid potentially life-threatening complications such as pulmonary hemorrhage [1, 8–10]. Using these safety measures periinterventional mortality is actually 0–1.8% and similar to the risk of PEA when performed in experienced centers [1, 10–14].

Existing methods for BPA treatment monitoring are the use of an intraluminal pressure wire, optical coherence tomography, intravascular ultrasound during the intervention, transthoracic echocardiography, right-sided heart catheterization (RHC) and 2D-perfusion angiography [15–18]. Also, the N-terminal pro B-type natriuretic peptide (NT-proBNP) concentration can be used to predict long-term outcomes and guide management of patients and treatment decisions in patients with inoperable CTEPH or persistent or recurrent pulmonary hypertension after PEA [19–22]. However, none of the above methods quantifies pulmonary parenchymal blood flow with full lung coverage as well as cardiac mass and function in a single diagnostic "one-stop-shop" examination.

In recent years, cardio-pulmonary MRI has shown its ability to evaluate pulmonary hemodynamics, cardiac function and pulmonary parenchymal perfusion noninvasively in patients with CTEPH after PEA and after completion of BPA treatment with multiple sessions [8, 23–27]. However, it is currently unknown if cardio-pulmonary MRI is sensitive enough to detect changes after a single BPA treatment session.

Therefore, the aim of this study was to determine cardio-pulmonary hemodynamic changes after a single BPA treatment session in patients with inoperable CTEPH by using non-invasive functional cardio-pulmonary MRI measurements.

Methods

Patient cohort

This retrospective study was approved by the institutional ethics review board. Written informed consent was obtained from all patients. Between June 2014 and September 2016 46 CTEPH patients were considered to be inoperable by local CTEPH-board (interdisciplinary conference of pneumology, cardiothoracic surgery and radiology) decision and underwent BPA treatment. Location of thrombi, surgical accessibility, age and/or comorbidity were parameters for treatment decision. Based on the NICE criteria, diagnosis of CTEPH was based on medical history, physical examination, electrocardiogram (ECG), chest X-ray, echocardiography, lung ventilation/perfusion scintigraphy, right heart catheterization (RHC) and pulmonary artery angiography [28]. Of these, only 33 patients were referred for a cardio-pulmonary MRI (Fig. 1). MRI was performed 1 day before the first BPA treatment session and 62 (51; 82) (median [25th, 75th percentile]) days after the first BPA treatment session (Table 1). There was no additional BPA treatment session between the two MRIs.

Six-minute walking distance (6MWD) and New York Heart Association functional classification (NYHA FC) were evaluated before and 63 (44; 98) days after BPA. NT-proBNP

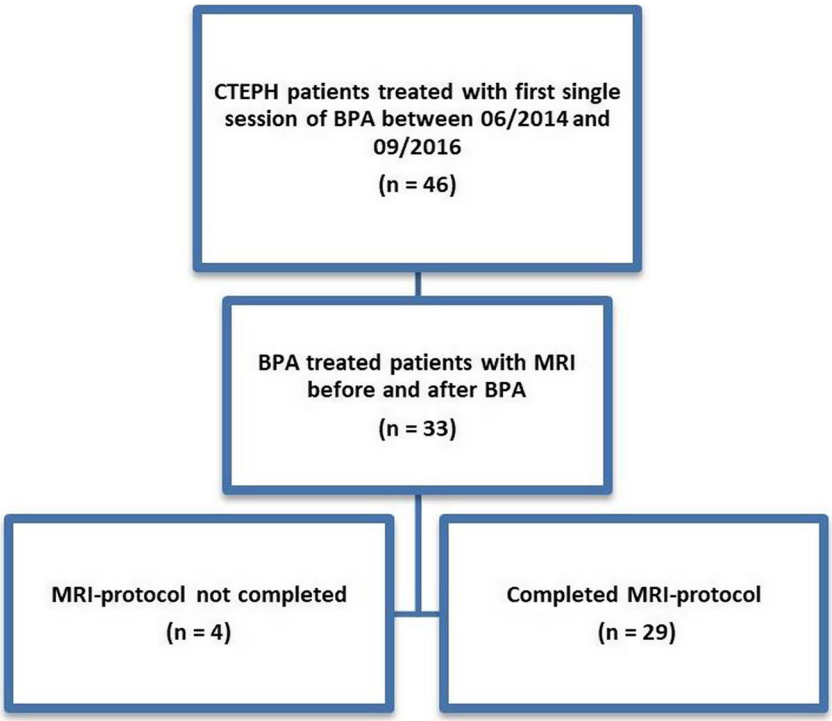

Fig. 1 Flowchart of the patient cohort. CTEPH, chronic thromboembolic pulmonary hypertension; BPA, balloon pulmonary angioplasty

was assessed at baseline and 61 (47; 79) days after BPA. Mean pulmonary artery pressure (mPAP) and pulmonary vascular resistance (PVR) were evaluated pre BPA by RHC.

BPA was performed as described by Hinrichs et al [7, 29] in supine position using a monoplane, ceiling-mounted angiography system equipped with a 30 × 40-cm-high dynamic range flat-panel detector (Artis Q; Siemens Healthineers, Forchheim, Germany). Medical treatment and time intervals between initial CTEPH diagnosis and BPA were determined from the medical records.

Table 1 Patient population information with completed MR imaging protocol

Parameter	Total $n = 29$
Age (years)	72 (60; 77)
Females	18
BSA	1.83 (1.64; 2.04)
Interval between first MRI and BPA (days)	1 (1; 1)
Interval between BPA and second MRI (days)	62 (51; 82)
Interval between RHC and BPA (days)	83 (71; 111)
Interval between pre-intervention sampling of N-terminal pro B-type natriuretic peptide and BPA (days)	1 (1; 2)
Interval between BPA and sampling of N-terminal pro B-type natriuretic peptide (days)	61 (47; 79)
Treated segments total	3 (2; 4)
Treated segments in the right lower lobe	3 (2; 3)
Treated segments in the left lower lobe	3 (3; 4)
Treated segments in the middle lobe	2 and 2
Number of balloon dilatations during BPA session	4 (3; 5)

Median (24th; 75th percentile)

BSA body surface area, *BPA* balloon pulmonary angioplasty, *RHC* right heart catheterization

MRI examination

All patients underwent lung MRI at 1.5 T (Avanto or Aera, Siemens Healthineers). CTEPH-related changes of regional lung perfusion were evaluated by three-dimensional dynamic contrast-enhanced (DCE) time-resolved angiography with stochastic trajectories (TWIST) [30] using an 8-channel torso phased array coil and the following MR imaging parameters: TE 0.7 ms; TR 2.1 ms; flip angle 25°; 40 three-dimensional data sets with an update rate of 1.0–1.2 s; acquisition matrix 192 × 113; field of view 50 cm × 42 cm; 0.04 mmol/kg gadoteric acid at 5cc/s i.v.; 30-36 reconstructed coronal slices (slice thickness 6 mm) covering the whole lung were acquired in a single breath hold.

Cardiac function was evaluated by retrospectively ECG-gated cine balanced steady-state free precession sequences during short inspiratory breath holds using short-axis views covering the whole heart with following MRI parameters: TE 1 ms; TR 2.9 ms; flip angle 75°; slice thickness 8 mm; field of view 290 × 360 mm^2; matrix size 208 × 256; temporal resolution 35 ms; in-plane resolution 1.4 × 1.4 mm^2; bandwidth/pixel 540 Hz/pixel; 30 reconstructed phases.

MR data analysis

The MR data analysis was performed by two trained observers (1 and 5 years of cardio-pulmonary MRI experience) performing one consensus read, blinded to the localization of BPA treatment and clinical parameters. After all MR data were analyzed and the MR data bank closed, the observers were un-blinded to the BPA treatment and clinical data. First-pass DCE MRI images were used for calculating parenchymal microvascular pulmonary blood flow (PBF) maps by using a pixel-by-pixel deconvolution analysis with dedicated software (PMI-MIKE 0.4, Platform for Research in Medical Imaging) [31, 32]. Arterial input function was derived with a region of interest in the main pulmonary artery. Regions of interest were drawn on the lung perfusion maps excluding larger pulmonary vessels. Mean parenchymal PBF was calculated for the total lung and for each lobe.

First-pass bolus kinetic parameters were determined on the DCE-MR images. One region of interest was placed in the right ventricular (RV) and left ventricular (LV) cavities, including as much blood pool as possible without extending into the myocardium, papillary muscles or trabeculations. Time-intensity curves were generated for passage of the contrast material bolus through the regions of interest by using average signal intensity. First-pass bolus kinetic parameters were derived from these curves: Right-to-left ventricle pulmonary transit time (PTT) was calculated by subtracting the time of peak enhancement in the RV from that in the LV. Time to peak (TTP) was calculated in the LV cavity as the interval from the first appearance of the contrast material bolus to its peak signal intensity, where first appearance was defined as the time of 20% peak signal intensity. Full width at half maximum (FWHM) was defined in the LV cavity as width of the time-intensity curve at half its maximum signal intensity [27, 33].

Short-axis cine MR images were analyzed with dedicated cardiac software (CVI42 software, Circle Cardiovascular Imaging Inc.). Cine images were analyzed by semiautomated contour detection for LV and RV endo- and epicardial contours in end-diastole and end-systole by one experienced radiologist (5 years of cardiac MRI experience). Papillary muscles as well as myocardial trabeculations were included in the blood pool [34]. Manual corrections were performed if necessary. Using short-axis cine images, the following parameters were evaluated for the LV and the RV: stroke volume (SV), ejection fraction (EF), end-diastolic volume (EDV) and end-systolic volume (ESV), myocardial mass, systolic/diastolic eccentricity indices (ecc.ind.) [35], interventricular septal angle, interventricular septal angle ratio and ventricular mass index (RV mass/LV mass; VMI) [36, 37]. Volumes and masses were normalized to body surface area (BSA).

MRI-derived mPAP was calculated as described by Swift et al using the following formula: MRI-derived mPAP = -4.6 + (interventricular septal angle × 0.23) + (ventricular mass index × 16.3) [37].

Statistical analysis

Statistical analysis was performed with JMP Pro 13 software (SAS Institute,). All values are given as median and (25th; 75th) percentiles. Shapiro-Wilk test was performed to test normality of distribution. Since many of the tested variables were not normally distributed, nonparametric tests were used. For comparison of values pre- and post-BPA, a paired two-sided Wilcoxon rank sum test was performed. Spearman rho correlation was used for descriptive univariate analysis. Multiple linear regression analysis was implemented to estimate the relationship of PBF change in the treated lobe with treatment change of FWHM, CO, VMI, PTT and PBF change in the non-treated lobes. A comparison between RHC- and MRI-derived mPAP was performed using Pearson's correlation and a paired t-test. $P < 0.05$ was considered indicative of a statistically significant difference.

Results

Overall, 29 of 33 CTEPH patients (72 [60;77] years; 13 male; 20 female) completed the MRI protocol without any side effects. Four patients were excluded from the study because of an incomplete MRI protocol (one for extravasation during injection of contrast agent, two for contraindication for contrast agents due to renal failure and one for incomplete study due to claustrophobia, Fig. 1). At first BPA the right lower lobe was predominantly treated (22 patients, 3 [2; 3] treated segments, Fig. 2) followed by the left lower lobe (5 patients, 3 [3; 4] treated segments). The middle lobe was treated in two patients (2 treated segments). Two lobes (middle and right lower lobe) were treated only in one patient during the initial BPA session (total treated segments: 4). No interventional treatment was performed in the upper lobes in our cohort at time of first BPA. Twenty-seven of 29 patients were receiving PH medication before, during and after BPA; see Table 2.

Two months after BPA, regional PBF increased in the total lung parenchyma ($p = 0.005$), treated ($p < 0.0001$) and non-treated lobes ($p = 0.015$) (Table 3). The PBF treatment changes in the treated lobe were significantly larger than in the non-treated lobes ($p = 0.0049$): the post/pre PBF ratio of the treated lobes was 1.24 (1.08; 1.62), and the post/pre PBF ratio of the non-treated lobes was 1.15 (0.96; 1.33). The post/pre PBF ratio of the treated lobes highly correlated with the post/pre PBF ratio of the non-treated lobes ($r = 0.77$, $p < 0.0001$, Table 4).

First-pass bolus kinetic parameters improved after the BPA and LV mass increased ($p = 0.0007$). No significant differences were observed for biventricular volumes after a single BPA treatment session for the whole cohort. The systolic eccentricity index decreased from 1.7 to 1.5 ($p = 0.042$). MRI-

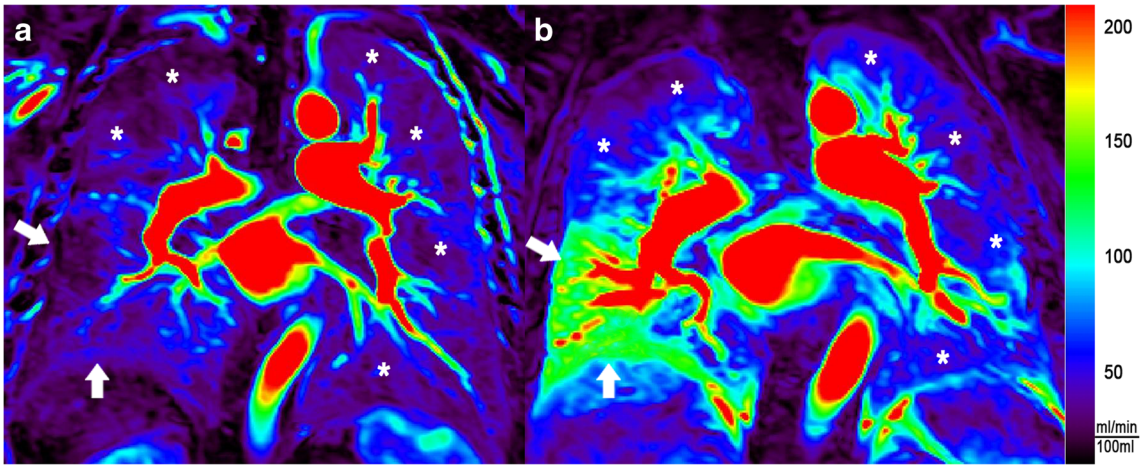

Fig. 2 Pulmonary parenchymal blood flow (PBF) maps of a 75-year-old male with inoperable chronic thromboembolic pulmonary hypertension who underwent lung MRI before (**a**) and 53 days after successful balloon pulmonary angioplasty (BPA) (**b**). After a single BPA session treating three segments (8, 9 and 10) in the right lower lobe, a marked increase of PBF was observed in this lobe (arrows) (median PBF 26.5 to 103.3 ml/min/100 ml). Also a notably milder increase of PBF in the non-treated lobes (*) (median PBF 24.2 to 41.0 ml/min/100 ml) was depicted, likely due to a combination of improved RV function (RV-EF pre 31%, post 37%) caused by decreased pulmonary pressure (MRI-derived mPAP pre 68 mmHg, post 59 mmHg) leading to clearly improved cardio-pulmonary hemodynamics (PTT pre 13.1 s, post 8.8 s) as well as continued medical therapy (riociguat)

derived mPAP decreased (40 to 37 mmHg; $p = 0.022$). There was a trend toward lower NT-proBNP levels for the whole cohort ($p = 0.054$). NYHA FC scores were significantly lower after BPA ($p = 0.0079$).

To assess the relationship of PBF changes with cardiac, hemodynamic changes, Spearman rho correlations showed that changes in FWHM, CO and VMI correlated with PBF changes in the treated lobe and non-treated lobes. In addition, changes in NT proBNP, MRI-derived mPAP, PTT, RV EF, RV SV and PBF in the non-treated lobes correlated with PBF changes only in the treated lobe (Table 4).

To determine whether changes in PBF in the treated lobe are more strongly predicted by changes in first-pass bolus kinetic parameters or cardiac parameters, a multivariate model was implemented, including FWHM, PTT, CO and VMI, as independent parameters. PBF changes in the treated lobe were independently predicted by PTT (Table 5a). In a second step, PBF change in the non-treated lobes was added to the model: PBF changes in the treated lobe were independently predicted by PTT as well as PBF change in the non-treated lobes (Table 5b).

Pre-interventional MRI-derived mPAP and RHC-derived mPAP showed a strong linear correlation (Pearson's correlation coefficient $r = 0.79$; $p < 0.0001$) with a slight bias toward higher values of MRI-derived mPAP (mean difference 4.8 mmHg, [95% CI 1.7-7.7 mmHg], p = 0.003, paired t-test).

Discussion

The main findings of the presented study were that PBF improved in the treated lobes and to a lesser degree in the non-treated lobes for the whole cohort after a single BPA session treating a median of three segments. Hemodynamic improvement was observed by improvement of first-pass bolus kinetic parameters and MRI-derived mPAP. PBF changes in the treated lobe were independently predicted by PTT as well as PBF change in the non-treated lobes.

Improvement of regional parenchymal PBF and pulmonary hemodynamics is the main purpose of BPA treatment [3]. In accordance, we were able to show a significant increase of PBF in the treated lobes after a single BPA treatment session

Table 2 Pulmonary hypertension medication of the patient cohort

Medication at time of second MRI*	No. of patients	Administration period before BPA (days)	Total administration period until 2nd MRI (days)
Riociguat	13	188 (89; 480)	295 (139; 545)
Sildenafil or tadalafil	12	682 (155; 1391)	751 (219; 1465)
Sildenafil or tadalafil and bosentan or ambrisentan	2	996 and 2464	1068 and 2505

Median (24th; 75th percentile)

*Two patients had no medication for pulmonary hypertension during the study period

Table 3 Changes in parenchymal pulmonary blood flow (PBF), first-pass bolus kinetic parameters, cardiac function, morphology and physical status before and after balloon pulmonary angioplasty (BPA)

Parameter	Pre BPA	Post BPA	*p* value
PBF in total lung (ml/min/100 ml)	28 (21; 34)	33 (26; 38)	0.0053
PBF in treated lobe (ml/min/100 ml)	31 (22; 39)	41 (33; 48)	< 0.0001
PBF in non-treated lobes (ml/min/100 ml)	28 (21; 32)	33 (25; 36)	0.015
PTT (s)	9.0 (8.0; 9.9)	8.1 (7.0; 9.6)	0.0049
TTP (s)	6.1 (4.5; 7.0)	5.2 (4.5; 6.3)	0.0047
FWHM (s)	14.6 (11.2; 20.2)	13.0 (9; 15.6)	0.028
Heart frequency (/min)	70 (57; 80)	67 (58; 77)	0.55
CO (l/min)	4.8 (4.1; 5.7)	5.0 (4.3; 5.8)	0.32
LV-EDV/BSA (ml/m^2)	64 (55; 70)	68 (60; 75)	0.11
LV-ESV/BSA (ml/m^2)	22 (18; 30)	25 (18; 31)	0.46
LV-SV/BSA (ml/m^2)	42 (31; 46)	43 (36; 47)	0.18
LV-EF (%)	63 (58; 67)	64 (56; 69)	0.79
LV-diastolic-mass/BSA (g/m^2)	53 (48; 66)	59 (54; 66)	0.0007
RV-EDV/BSA (ml/m^2)	90 (72; 115)	90 (74; 117)	0.9
RV-ESV/BSA (ml/m^2)	42 (31; 76)	46 (30; 75)	0.33
RV-SV/BSA (ml/m^2)	43 (32; 50)	44 (37; 52)	0.48
RV-EF (%)	51 (36; 57)	50 (37; 59)	0.077
RV-diastolic-mass/BSA (g/m^2)	35 (26; 52)	36 (26; 52)	0.83
Ventricular mass index	0.56 (0.48; 0.94)	0.57 (0.45; 0.83)	0.23
Systolic eccentricity index	1.7 (1.4; 2.1)	1.5 (1.2; 1.8)	0.042
Diastolic eccentricity index	1.2 (1.1; 1.4)	1.2 (1.1; 1.3)	0.36
Interventricular septal angle (°)	155 (125; 189)	145 (124; 187)	0.14
Interventricular septal angle ratio	1.9 (1.6; 2.3)	2.0 (1.6; 2.2)	0.86
MRI-derived mPAP (mmHg)	40 (33; 51)	37 (32; 53)	0.022
mPAP (mmHg)	39 (26; 49)	-	-
Pulmonary vascular resistance (dynes × sec × cm^{-5})	582 (294; 855)	-	-
Six-minute walking distance (m)*	372 (242; 425)	360 (251; 429)	0.92
New York Heart Association functional score**	3 (3; 3)	3 (2; 3)	0.0079
N-terminal pro B-type natriuretic peptide (ng/l)	591 (247; 2220)	523 (222; 1487)	0.054

Median (24th; 75th percentile)

CO cardiac output, *PTT* pulmonary transit time *TTP* time to peak, *FWHM* full width at half maximum, *LV* left ventricular, *EDV* end-diastolic volume, *BSA* body surface area, *ESV* end-systolic volume, *SV* stroke volume, *EF* ejection fraction, *RV* right ventricular, *mPAP* mean pulmonary artery pressure

*Complete 6-min walking distance data were available pre and post BPA only for 25 patients

**Complete New York Heart Association functional score data were available pre BPA and post BPA only for 28 patients

using quantitative DCE-MRI. In addition, a significant increase of PBF was observed in the non-treated lobes. The observed changes in the non-treated lobes may be explained by improvements of global cardio-pulmonary hemodynamics after a single BPA treatment session, which is supported by decreased MRI-derived mPAP measurements and improved PTT. Also continued medical treatment may have contributed to these effects. After 3-month treatment with a soluble guanylate cyclase stimulator (riociguat), significantly reduced right heart size and improved RV function and CO in PAH and CTEPH were reported in a previous study [38]. Therefore, the observed changes in PBF are likely due to a combination of BPA and medical therapy, because the PBF changes in the treated lobe were significantly higher compared with the non-treated lobes.

Increased LV-EDV and LV mass were reported after BPA treatment in combination with medical therapy using cardiac MRI [8]. In this study Sato et al showed improvement of biventricular function and flow dynamics in the pulmonary artery in a cohort of 30 CTEPH patients after completion of BPA treatment with several BPA sessions (a mean of 5 BPA sessions per patient) in combination with medial therapy [8]. In the present study, we observed no significant changes of RV mass and function for the whole cohort. However, changes in CO, RV-EF, RV-SV and VMI correlated with changes in PBF in the treated lobe after one single BPA treatment session.

Table 4 Univariate correlation analysis using Spearman rho correlation

	PBF ratio whole lung		PBF ratio treated lung		PBF ratio non-treated lung	
Parameter ratios	r	*p*	r	*p*	r	*p*
Six-minute walking distance (m)*	0.03	0.98	-0.12	0.58	0.04	0.84
New York Heart Association functional score	0.10	0.62	0.22	0.27	0.09	0.65
N-terminal pro B-type natriuretic peptide	-0.24	0.21	-0.38	0.040*	-0.18	0.35
MRI-derived mPAP	-0.33	0.079	-0.42	0.024*	-0.29	0.13
PTT	-0.10	0.61	-0.48	0.0098*	-0.09	0.63
TTP	-0.31	0.11	-0.36	0.059	-0.28	0.15
FWHM	-0.64	0.0002*	-0.63	0.0004*	-0.62	0.0005*
LV-EF	0.18	0.35	0.22	0.26	0.076	0.69
CO	0.47	0.0093*	0.47	0.0102*	0.40	0.0304*
LV-HF	0.07	0.72	0.07	0.72	0.10	0.60
LV-EDV/BSA	0.12	0.55	0.10	0.62	0.14	0.48
LV-ESV/BSA	-0.12	0.53	-0.062	0.75	-0.05	0.80
LV-SV/BSA	0.35	0.061	0.36	0.05	0.28	0.15
LV-diastolic-mass/BSA	0.32	0.089	0.26	0.17	0.23	0.23
RV-EF	0.30	0.12	0.47	0.0104*	0.24	0.20
RV-diastolic-mass/BSA	-0.11	0.58	-0.10	0.60	-0.17	0.38
RV-EDV/BSA	0.20	0.31	0.11	0.56	0.17	0.39
RV-ESV/BSA	-0.10	0.60	-0.22	0.26	-0.07	0.71
RV-SV/BSA	0.33	0.078	0.39	0.0372*	0.27	0.15
RV-diast.-Masse/BSA	-0.14	0.48	-0.12	0.54	-0.19	0.32
VMI	-0.41	0.026*	-0.45	0.0134*	-0.41	0.0268*
Systolic eccentricity index	-0.20	0.29	-0.30	0.11	-0.2	0.30
Alpha septal angle	-0.03	0.86	-0.13	0.51	0.03	0.89
PBF non-treated lung			0.77	< 0.0001*		

Ratio postBPA/pre BPA, *CO* cardiac output, *PTT* pulmonary transit time, *TTP* time to peak, *FWHM* full width at half maximum, *LV* left ventricular, *EDV* end-diastolic volume, *BSA* body surface area, *ESV* end-systolic volume, SV stroke volume, *EF* ejection fraction, *RV* right ventricular, *mPAP* mean pulmonary artery pressure, *VMI* ventricular mass index, *MRI* magnetic resonance imaging, *PBF* parenchymal pulmonary blood flow

*Significant values: $p < 0.05$

This is likely due to reduced pulmonary vascular resistance as shown by reduced MRI-derived mPAP after treatment, which leads to improved RV function and CO. Also improved lung parenchymal perfusion and CO cause an increased preload to the LV, which leads to increased LV-EDV and LV mass [8]. This could explain the changes in VMI in our study, which correlated with changes in PBF in the treated lobe.

We observed improvement of systolic eccentricity indices for the whole cohort. As the systolic eccentricity index correlates with mPAP [39], septal flattening is part of the MRI-based prediction model for estimation of mPAP proposed by Swift et al [37]. MRI-derived pressures were strongly correlated with RHC-measured mPAP in our cohort. As there was only a small bias toward higher values using MRI-derived mPAP, we conclude that this parameter is a valid noninvasive alternative to measure mPAP in patients with CTEPH.

We were able to detect a significant improvement of first-pass bolus kinetic parameters (PTT; TTP, FWHM) after a single BPA treatment session. These parameters are known MR biomarkers for pulmonary hemodynamics, cardiac function and ventricular remodeling and predict mortality in patients with pulmonary hypertension [33, 40]. PBF changes in the treated lobe were independently predicted by PTT as well as PBF change in the non-treated lobes. Hence, PTT may be utilized as an MRI parameter to determine treatment response after BPA in the future.

One important limitation of our study is that our sample size was relatively small and the number of explored MRI parameters was relatively large. Nevertheless, we do not assume that the sample size substantially affected the main conclusion of this exploratory study. We also acknowledge that no RHC-derived mPAP was available after first BPA. However,

Table 5 Multiple linear regression analysis

Parameter	Post/pre PBF ratio treated lobe			
	β	95% Confidence Interval		*p*
Model 1				
5a				
FWHM ratio	-0.03	-0.81	0.75	0.94
CO ratio	0.91	-0.06	1.87	0.06
VMI ratio	-0.61	-1.72	0.50	0.26
PTT ratio	-1.67	-3.26	-0.08	0.04*
Model 2				
5b				
FWHM ratio	0.45	-0.23	1.12	0.18
CO ratio	0.24	-0.61	1.09	0.56
VMI ratio	-0.3	-1.2	0.6	0.5
PTT ratio	-2.35	-3.67	-1.03	0.0013*
PBF ratio non-treated lobes	0.98	0.44	1.52	0.001*

The first model (5a) included FWHM, CO, VMI and PTT changes to predict changes in PBF in the BPA-treated lobe. In a second model (5b), PBF changes in the non-treated lobes were added to the first model. The N-terminal pro B-type natriuretic peptide and right ventricular ejection fraction were excluded from the model because of significant cross correlations with PTT. Right ventricular stroke volume was excluded from the model because of significant cross correlation with CO. MRI-derived mean pulmonary artery pressure (mPAP) was excluded, because VMI is part of the MRI-derived mPAP calculations. Using MRI-derived mPAP instead of VMI did not change the model results.

Ratio postBPA/pre BPA, *CO* cardiac output, *PTT* pulmonary transit time, *FWHM* full width at half maximum, *VMI* ventricular mass index, *MRI* magnetic resonance imaging, *PBF* parenchymal pulmonary blood flow

*Significant values: $p < 0.05$

we were able to evaluate and quantify effects on pulmonary pressure by using MRI-derived mPAP with good agreement with RHC-derived mPAP before the first BPA. We performed segmentation of whole lobes for anatomic consistency and better interpatient comparison, although not all segments of a lobe were treated. This may have led to an underestimation of the local treatment effect of the treated segments. Nevertheless, we could detect significant changes after a single BPA treatment session. All except two CTEPH patients with borderline elevated mPAP in the presented BPA cohort received medical treatment according to the current CTEPH treatment guidelines [28]. Treatment of patients with inoperable CTEPH is a multi-modal therapy including medical and interventional therapy at least until BPA treatment is completed and pulmonary pressures have normalized. The two patients without medical treatment showed a 10% and 5% PBF improvement of the treated lobe and 8% and 2% PBF improvement of the non-treated lobes, respectively.

In conclusion, the combination of regional pulmonary parenchymal perfusion and cardiac MRI is a feasible, noninvasive "one-stop-shop" examination to evaluate treatment response of patients with CTEPH after a single BPA treatment session.

Funding This study has received funding from the German Center for Lung Research (DZL).

Compliance with ethical standards

Guarantor The scientific guarantor of this publication is Prof. Dr. Jens Vogel-Claussen.

Conflict of interest The authors of this manuscript declare no relationships with any companies, whose products or services may be related to the subject matter of the article.

Statistics and biometry One of the authors has significant statistical expertise.

Informed consent Written informed consent was obtained from all subjects (patients) in this study.

Ethical approval Institutional Review Board approval was obtained.

Methodology
- retrospective
- observational
- performed at one institution

References

1. Olsson KM, Wiedenroth CB, Kamp JC et al (2017) Balloon pulmonary angioplasty for inoperable patients with chronic thromboembolic pulmonary hypertension: the initial German experience. Eur Respir J 49:1602409. https://doi.org/10.1183/13993003.02409-2016
2. Lang IM, Madani M (2014) Update on chronic thromboembolic pulmonary hypertension. Circulation 130:508–518. https://doi.org/10.1161/CIRCULATIONAHA.114.009309
3. Hoeper MM, Madani MM, Nakanishi N, Meyer B, Cebotari S, Rubin LJ (2014) Chronic thromboembolic pulmonary hypertension. Lancet Respir Med 2:573–582. https://doi.org/10.1016/S2213-2600(14)70089-X
4. Kim NH, Delcroix M, Jenkins DP et al (2013) Chronic thromboembolic pulmonary hypertension. J Am Coll Cardiol 62:D92–D99. https://doi.org/10.1016/j.jacc.2013.10.024
5. Pepke-Zaba J, Delcroix M, Lang I et al (2011) Chronic thromboembolic pulmonary hypertension (CTEPH): results from an international prospective registry. Circulation 124:1973–1981. https://doi.org/10.1161/CIRCULATIONAHA.110.015008
6. Hoeper MM (2016) Residual Pulmonary hypertension after pulmonary endarterectomy: the fog is clearing. https://doi.org/10.1161/CIRCULATIONAHA.116.022595
7. Hinrichs JB, Renne J, Hoeper MM, Olsson KM, Wacker FK, Meyer BC (2016) Balloon pulmonary angioplasty: applicability of C-Arm CT for procedure guidance. Eur Radiol 26:4064–4071. https://doi.org/10.1007/s00330-016-4280-z
8. Sato H, Ota H, Sugimura K et al (2016) Balloon pulmonary angioplasty improves biventricular functions and pulmonary flow in chronic thromboembolic pulmonary hypertension. Circ J 80:1470–1477. https://doi.org/10.1253/circj.CJ-15-1187

9. Ogo T, Fukuda T, Tsuji A et al (2017) Efficacy and safety of balloon pulmonary angioplasty for chronic thromboembolic pulmonary hypertension guided by cone-beam computed tomography and electrocardiogram-gated area detector computed tomography. Eur J Radiol 89:270–276. https://doi.org/10.1016/j.ejrad.2016.12.013
10. Mizoguchi H, Ogawa A, Munemasa M, Mikouchi H, Ito H, Matsubara H (2012) Refined balloon pulmonary angioplasty for inoperable patients with chronic thromboembolic pulmonary hypertension. Circ Cardiovasc Interv 5:748–755. https://doi.org/10.1161/CIRCINTERVENTIONS.112.971077
11. Mayer E, Jenkins D, Lindner J et al (2011) Surgical management and outcome of patients with chronic thromboembolic pulmonary hypertension: Results from an international prospective registry. J Thorac Cardiovasc Surg 141:702–710. https://doi.org/10.1016/j.jtcvs.2010.11.024
12. Jenkins DP, Madani M, Mayer E et al (2013) Surgical treatment of chronic thromboembolic pulmonary hypertension. Eur Respir J 41:735–742. https://doi.org/10.1183/09031936.00058112
13. Shimura N, Kataoka M, Inami T et al (2015) Additional percutaneous transluminal pulmonary angioplasty for residual or recurrent pulmonary hypertension after pulmonary endarterectomy. Int J Cardiol 183C:138–142. https://doi.org/10.1016/j.ijcard.2015.01.034
14. Inami T, Kataoka M, Shimura N et al (2014) Pressure-wire-guided percutaneous transluminal pulmonary angioplasty: a breakthrough in catheter-interventional therapy for chronic thromboembolic pulmonary hypertension. JACC Cardiovasc Interv 7:1297–1306. https://doi.org/10.1016/j.jcin.2014.06.010
15. Champion HC, Michelakis ED, Hassoun PM (2009) Comprehensive invasive and noninvasive approach to the right ventricle-pulmonary circulation unit: state of the art and clinical and research implications. Circulation 120:992–1007. https://doi.org/10.1161/CIRCULATIONAHA.106.674028
16. Roik M, Wretowski D, Łabyk A et al (2016) Refined balloon pulmonary angioplasty driven by combined assessment of intra-arterial anatomy and physiology - Multimodal approach to treated lesions in patients with non-operable distal chronic thromboembolic pulmonary hypertension - Technique, safety and efficacy of 50 consecutive angioplasties. Int J Cardiol 203:228–235. https://doi.org/10.1016/j.ijcard.2015.10.116
17. Maschke SK, Renne J, Werncke T et al (2017) Chronic thromboembolic pulmonary hypertension: Evaluation of 2D-perfusion angiography in patients who undergo balloon pulmonary angioplasty. Eur Radiol 27:4264–4270. https://doi.org/10.1007/s00330-017-4806-z
18. Roik M, Wretowski D, Łabyk A et al (2017) Refined balloon pulmonary angioplasty-A therapeutic option in very elderly patients with chronic thromboembolic pulmonary hypertension. J Interv Cardiol. https://doi.org/10.1111/joic.12387
19. Leuchte HH, El Nounou M, Tuerpe JC et al (2007) N-terminal probrain natriuretic peptide and renal insufficiency as predictors of mortality in pulmonary hypertension. Chest 131:402–409. https://doi.org/10.1378/chest.06-1758
20. Nagaya N, Nishikimi T, Uematsu M et al (2000) Plasma brain natriuretic peptide as a prognostic indicator in patients with primary pulmonary hypertension. Circulation 102:865–870
21. Simonneau G, D'Armini AM, Ghofrani HA et al (2016) Predictors of long-term outcomes in patients treated with riociguat for chronic thromboembolic pulmonary hypertension: data from the CHEST-2 open-label, randomised, long-term extension trial. Lancet Respir Med 4:372–380. https://doi.org/10.1016/S2213-2600(16)30022-4
22. Suntharalingam J, Goldsmith K, Toshner M et al (2007) Role of NT-proBNP and 6MWD in chronic thromboembolic pulmonary hypertension. Respir Med 101:2254–2262. https://doi.org/10.1016/j.rmed.2007.06.027
23. American College of Cardiology Foundation Task Force on Expert Consensus Documents, Hundley WG, Bluemke DA et al (2010) ACCF/ACR/AHA/NASCI/SCMR 2010 expert consensus document on cardiovascular magnetic resonance: a report of the American College of Cardiology Foundation Task Force on Expert Consensus Documents. J Am Coll Cardiol 55:2614–2662
24. Kreitner KF, Kunz RP, Ley S et al (2007) Chronic thromboembolic pulmonary hypertension—assessment by magnetic resonance imaging. Eur Radiol 17:11–21. https://doi.org/10.1007/s00330-006-0327-x
25. Peacock AJ, Vonk Noordegraaf A(2013) Cardiac magnetic resonance imaging in pulmonary arterial hypertension. Eur Respir Rev 22:526–534. https://doi.org/10.1183/09059180.00006313
26. Jenkins D, Mayer E, Screaton N, Madani M (2012) State-of-the-art chronic thromboembolic pulmonary hypertension diagnosis and management. Eur Respir Rev 21:32–39. https://doi.org/10.1183/09059180.00009211
27. Schoenfeld C, Cebotari S, Hinrichs J et al (2016) MR imaging-derived regional pulmonary parenchymal perfusion and cardiac function for monitoring patients with chronic thromboembolic pulmonary hypertension before and after pulmonary endarterectomy. Radiology 279:925–934. https://doi.org/10.1148/radiol.2015150765
28. Galiè N, Humbert M, Vachiery JL et al (2016) 2015 ESC/ERS Guidelines for the diagnosis and treatment of pulmonary hypertension: The Joint Task Force for the Diagnosis and Treatment of Pulmonary Hypertension of the European Society of Cardiology (ESC) and the European Respiratory Society (ERS): Endorsed by: Association for European Paediatric and Congenital Cardiology (AEPC), International Society for Heart and Lung Transplantation (ISHLT). Eur Heart J 37:67–119. https://doi.org/10.1093/eurheartj/ehv317
29. Hinrichs JB, Marquardt S, von Falck C et al (2016) Comparison of C-arm computed tomography and digital subtraction angiography in patients with chronic thromboembolic pulmonary hypertension. Cardiovasc Intervent Radiol 39:53–63. https://doi.org/10.1007/s00270-015-1090-7
30. Rajaram S, Swift AJ, Telfer A et al (2013) 3D contrast-enhanced lung perfusion MRI is an effective screening tool for chronic thromboembolic pulmonary hypertension: results from the ASPIRE Registry. Thorax 68:677–678. https://doi.org/10.1136/thoraxjnl-2012-203020
31. Sourbron S, Dujardin M, Makkat S, Luypaert R (2007) Pixel-by-pixel deconvolution of bolus-tracking data: optimization and implementation. Phys Med Biol 52:429–447. https://doi.org/10.1088/0031-9155/52/2/009
32. Ingrisch M, Dietrich O, Attenberger UI et al (2010) Quantitative pulmonary perfusion magnetic resonance imaging: influence of temporal resolution and signal-to-noise ratio. Invest Radiol 45:7–14. https://doi.org/10.1097/RLI.0b013e3181bc2d0c
33. Skrok J, Shehata ML, Mathai S et al (2012) Pulmonary arterial hypertension: MR imaging-derived first-pass bolus kinetic parameters are biomarkers for pulmonary hemodynamics, cardiac function, and ventricular remodeling. Radiology 263:678–687. https://doi.org/10.1148/radiol.12111001
34. Vogel-Claussen J, Finn JP, Gomes AS et al (2006) Left ventricular papillary muscle mass: relationship to left ventricular mass and volumes by magnetic resonance imaging. J Comput Assist Tomogr 30:426–432
35. Ryan T, Petrovic O, Dillon JC, Feigenbaum H, Conley MJ, Armstrong WF (1985) An echocardiographic index for separation of right ventricular volume and pressure overload. J Am Coll Cardiol 5:918–927

36. Vogel-Claussen J, Shehata ML, Lossnitzer D et al (2011) Increased right ventricular septomarginal trabeculation mass is a novel marker for pulmonary hypertension: comparison with ventricular mass index and right ventricular mass. Invest Radiol 46:567–575. https://doi.org/10.1097/RLI.0b013e31821b7041
37. Swift AJ, Rajaram S, Hurdman J et al (2013) Noninvasive Estimation of PA Pressure, Flow, and Resistance With CMR Imaging: Derivation and Prospective Validation Study From the ASPIRE Registry. JACC Cardiovasc Imaging 6:1036–1047. https://doi.org/10.1016/j.jcmg.2013.01.013
38. Marra AM, Egenlauf B, Ehlken N et al (2015) Change of right heart size and function by long-term therapy with riociguat in patients with pulmonary arterial hypertension and chronic thromboembolic pulmonary hypertension. Int J Cardiol 195:19–26. https://doi.org/10.1016/j.ijcard.2015.05.105
39. Yamasaki Y, Nagao M, Kamitani T et al (2016) Clinical impact of left ventricular eccentricity index using cardiac MRI in assessment of right ventricular hemodynamics and myocardial fibrosis in congenital heart disease. Eur Radiol 26:3617–3625. https://doi.org/10.1007/s00330-015-4199-9
40. Swift AJ, Telfer A, Rajaram S et al (2014) Dynamic contrast-enhanced magnetic resonance imaging in patients with pulmonary arterial hypertension. Pulm Circ 4:61–70. https://doi.org/10.1086/674882